Multi-parametric characterization of an experimental model of cancer cachexia

M-F. Penet[1], S. Nimmagadda[1], M. Gadiya[1], B. Krishnamachary[1], M. G. Pomper[1], and Z. M. Bhujwalla[1]
[1]JHU ICMIC Program, Russell H. Morgan Department of Radiology and Radiological Science, The Johns Hopkins University School of Medicine, Baltimore, MD, United States

Introduction: Cachexia is a complex metabolic and nutritional syndrome that is characterized by a massive loss of adipose tissue and skeletal mass. It is encountered in up to 50% of cancer patients and accounts for more than 20% of cancer related deaths. This complex multifactorial syndrome significantly impairs quality of life and response to treatment. The degree of cachexia is inversely correlated with the survival time of the patient, and often implies a poor prognosis. Currently, there is no known cure for cachexia, since mechanisms underlying its manifestation are not defined clearly enough to identify and design effective therapeutic strategies. Alterations in protein and amino acid metabolism appear to play major roles. Several mediators, produced either by the tumor or by the host itself, have been described as playing an important role in the disease, such as inflammatory cytokines (tumor necrosis factor-α, interleukins 1 and 6, interferon-γ), glucocorticoids, tumor-derived proteolysis-inducing factor and lipid-mobilizing factor. In the present studies we have used magnetic resonance imaging (MRI) to characterize the vascular properties of cachectic *vs.* non-cachectic tumors. We have also analyzed the glucose metabolism of these tumors by using [^{18}F]fluorodeoxyglucose (FDG) with positron emission tomography (PET). These studies will provide further insight into the 'cachectic phenotype', which will be used to define new targets and improve treatment to arrest or reverse this condition.

Methods: In our studies, we used cachectic (MAC16) and non-cachectic (MAC13) murine colon adenocarcinoma tumors. MAC16 tumors induce extensive weight loss in tumor-bearing animals, whereas MAC13 tumors, although histologically similar to MAC16 tumors, do not induce weight loss. The MAC16 and MAC13 cell lines, originally from Dr. Tisdale's laboratory (Birmingham, UK), were obtained from Dr. Sidransky with Dr. Tisdale's permission. Cells (2 x 10^6 in 0.05 ml of Hanks balanced salt solution) were inoculated in the flank of male SCID mice. MRI studies were performed on a 4.7T Bruker Avance spectrometer using a home-built solenoid coil placed around the tumors. Mice were anesthetized with an intraperitoneal (i.p.) injection of ketamine and acepromazine. For vascular imaging, the tail vein was catheterized before placing the animal in the spectrometer. Multislice relaxation rate ($1/T_1$) maps were obtained by a saturation recovery method combined with fast T_1 SNAPSHOT-FLASH imaging. An M_0 map with a recovery delay of 7 s was initially acquired from four 1 mm thick slices through the tumor with an in-plane resolution of 0.125 mm followed by corresponding images obtained with three relaxation delays (100 ms, 500 ms, and 1 s) to derive quantitative T_1 maps. These T_1 maps were obtained before intravenous (i.v.) administration of albumin-GdDTPA (dose of 500 mg/kg) and repeated over a 21 minute period, starting 3 min after the injection. At the end of the imaging studies, the T_1 of the blood was measured. Data were processed using Interactive Data Language (IDL, Research Systems, Boulder, CO). For PET imaging, mice fasted overnight were injected with 200 μCi of FDG and. At 60 min post injection of the tracer, a 15 min static image was acquired over the tumors. Images were decay corrected and reconstructed using 2D OSEM (Ordered Subset Expectation Maximization). Image analysis was performed using AMIDE software.

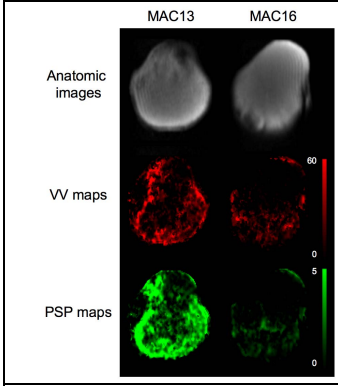

Figure 1: Representative anatomic images, vascular volume (VV) maps, and permeability surface area product (PSP) maps of a MAC13 and a MAC16 tumor.

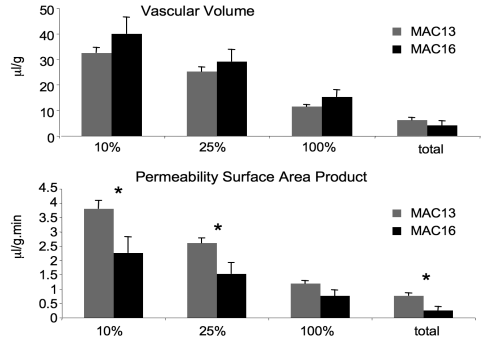

Figure 2: Vascular volume and PSP values of MAC13 and MAC16 tumors. The histograms represent analysis of the highest 10%, 25%, and all non-zero values. The total values represent the all non-zero values multiplied by the fractional area occupied by the values. Mean ± sem, n = 5, *P < 0.05.

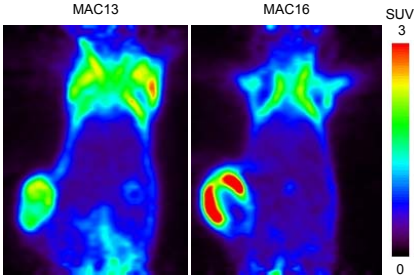

Figure 3: PET imaging of FDG uptake in MAC13 and MAC16 tumors (SUV: standard uptake value)

Results and Discussion: The non-cachectic (MAC13) and cachectic (MAC16) murine colon adenocarcinoma tumors were both palpable within one week of inoculation. Cachectic MAC16 tumors induced extensive weight loss, unlike the non-cachectic MAC13 tumors. The difference in the weight of mice became significant within 2 weeks after inoculation. Mice with comparable tumor volumes were imaged 3 to 4 weeks after inoculation, by which time the mean weight of the MAC16 tumor bearing mice was significantly lower than the mean weight of the MAC13 tumor bearing mice. Representative vascular volume and permeability maps of MAC13 and MAC16 tumors are shown in Figure 1. While vascular volumes were not significantly different between the two groups, we did observe significantly lower permeability in the cachectic tumors (Figure 2). Consistent with the MRI data we found significantly lower levels of VEGF mRNA in quantitative-RT-PCR of tumor extracts of MAC16 tumors compared to MAC13 tumors but not in MAC16 cells compared to MAC13 cells (data not shown). FDG PET imaging revealed increased glycolytic activity in a cachectic MAC16 tumor compared to a non-cachectic MAC13 tumor (Figure 3). These studies are part of our ongoing work to obtain a comprehensive characterization of the 'cachectic phenotype' using noninvasive multi-modality imaging that will allow us to detect cancer-induced cachexia and identify new targets to prevent or reverse this condition.

This work was supported by NIH R21 CA140904, U24 CA92871 and P50 CA103175. We thank Mr. Gary Cromwell for maintaining the cell lines and inoculating the tumors, and Ms. Flonné Wildes for technical assistance.